TECHNICAL MEMORANDUM

237

A modified set up of the advection scheme in the ECMWF wave model

J-R. Bidlot, P. Janssen,
B. Hansen and H. Günther

Research Department

August 1997

European Centre for Medium-Range Weather Forecasts
Europäisches Zentrum für mittelfristige Wettervorhersage
Centre européen pour les prévisions météorologiques à moyen

A MODIFIED SET UP OF THE ADVECTION SCHEME IN THE ECMWF WAVE MODEL

Jean-Raymond Bidlot, Peter Janssen, Björn Hansen, Heinz Günther

ABSTRACT

The problem of unrealistic wave propagation behind islands and along axis directions was solved by rotating the mean direction of the directional spectral bins by half the bin width. It was therefore possible to reintroduce the small islands that had been removed when implementing the operational high resolution model. Comparison with the old scheme shows a local improvement in the representation of the shadow zone in the lee of islands. Unrealistic north-south swell propagations in narrow bands ("cigar-like structure") are also avoided. Aside from those localised improvements, global scores are fairly neutral. This was to be expected from the inherent limitations of the discrete advection scheme used in the wave model. The benefit is nevertheless sufficient to justify the implementation (at no cost) of the new scheme into the operational suite (on May 14th 1997, 12Z).

1. INTRODUCTION

While testing the high resolution version of the ECMWF Wave Model (WAM) in the Autumn of 1996, it soon became evident that there were problems regarding excessive shadowing behind islands. A typical example is shown in figure 1a which is reproduced from *Bidlot et al.* (1997). Note that in this example waves are coming from the North Pacific propagating almost from North to South. These waves hit Hawaii and a considerable shadow zone is formed behind Hawaii of several thousands of kilometres. Although shadowing does occur in nature it seems most unlikely that such an extensive shadow zone is realistic. Therefore for the operational suite it was decided to remove all the isolated islands (figure 1b). It is remarked that in the lower resolution model such problems did not occur because of the absence of islands.

The reason for the occurrence of the extensive shadow zone has to do with the choice of directional discretisation of the wave model spectrum. Choosing North as reference direction, the spectrum is discretised in 12 bins starting at 0° North. Hence all the waves in the first segment between -15° and +15° are supposed to propagate northward. Suppose that we have an almost unidirectional wave field propagating from the North, so that there is only wave energy in the seventh directional bin and suppose that this wave field hits an isolated island. The first gridpoint in the shadow zone of the island presumably has no energy. The question now is what happens to the second grid point which lies just south of the first one. The WAM model uses a first-order upwinding scheme and therefore only the 2 grid points in the upwind direction are considered (one per axis). In the case of southward propagation, only the grid point just North of the grid point in question is considered and due to the presence of the island, it has no energy. In addition, because the waves propagate along a meridian, the grid point in question will not receive energy from its neighbours to the right and to the left (there is no flow across the lateral sides of the grid box). As a result, the second grid point receives no energy and this argument applies to all the grid points in the shadow zone, therefore a large shadow zone is formed. Thus, the advection scheme has problems when waves are propagating along the meridian and to some extent along lines of constant latitude as well. The reason is the choice of directional discretisation of the spectrum. When waves are propagating along the axes of the chosen coordinate system no information is supplied by the left and right neighbours (i.e. there is no mixing of information) and, in fact it can be shown that the numerical group speed of the waves along those directions has a maximum. As a result the well-known garden-sprinkler effect occurs (*Swamp* 1985, *Booij and Holthuisen* 1987)

It should be clear that these problems are caused by the combination of the fairly crude discretisation of the wave spectrum and the first order upwind advection scheme. There are several possibilities to alleviate these problems, most of them are quite expensive. An elegant, inexpensive solution was suggested by Günther. His main idea was to make sure that in the numerical representation of the spectrum, propagation along the axis of the coordinate system is avoided. This may be achieved by simply rotating the wave spectrum by half the directional width. The resulting wave height field for the swell case near Hawaii is shown in figure 1c, while the difference between figure 1b and figure 1c is shown in figure 2. Rotation of the spectrum now results in a realistic looking wave height field (figure 1c), while the difference map of figure 2 reveals the typical plus-minus features of the garden-sprinkler effect. In addition it should be noted that these differences are quite large of the order of 1-2 metres. Although it turned out that the swell case of Hawaii in November 1996 was quite exceptional, a number of 10 day forecasts revealed typical differences between 0.25 and 1 m in wave height. Therefore, although the rotation of the spectrum is beneficial near islands, the question now is whether this change is detrimental to the scores or not.

Section 2 briefly summarises the implementation of the new scheme. We also present a few more examples which support the motivation behind this new scheme. An extensive e-suite was run for a period of over a month, the results of which are given in the section 3.

2. IMPLEMENTATION OF THE NEW SCHEME

The small software changes that were necessary to run WAM with the directional bins rotated by half the bin width can be found in appendix A. Please note that these modifications do not alter the direction of reference (North) but only use the value of half the bin width (15°) as the initial direction in the discretised spectrum definition.

The bathymetry was modified to contain all islands that had been removed in the operational setting (Bidlot et al. 1997). A few more islands were added manually by correcting the topographic data (see input to PREPROC). We have basically enhanced or added all the main Hawaiian Islands and as well as a few islands in the northern part of the North Sea (for the full list see appendix B). Finally, after discussion with the Irish Meteorological Services, we took the opportunity to also correct the bathymetry around the west coast of Ireland by adding sea points where the original topographic data had resulted in unrealistic land points. As an example, we have presented in figure 3 the new model grid around Europe.

A full e-suite experiment was run for the period of December 5th 1996 to January 17th 1997 following a 10-day warm-up run. This period corresponds to the first month of the operational high resolution run. Some of the usual verification tools were used to compare both e-suite and operational runs. Following the favourable results of this latter experiment, it was decided to implement these changes in both global and mediterranean operational models. This new implementation was put in place on April 15th, 1997 (starting from a cold start) and was run in parallel with the old operational model until May 13th, 1997, 12Z. After that time, the new implementation became fully operational.

Before looking at the global statistics of the e-suite, it is interesting to note how the new scheme is beneficial in preventing unrealistic north-south propagation. Figure 4 shows the operational wave forecast for December 8th 1996 (left panels). One can clearly see the elongated feature (cigar like) which propagates due South across most of the equatorial Atlantic Ocean without any sign of dispersion. In the e-suite run (right panels), there is indeed southward propagation of wave energy, but in a more diffuse manner, which seems more realistic. In the course of this one month experiment, 2 to 3 cigar-like features propagating across the equatorial Atlantic appeared in the operational runs and not in the e-suite. These differences might influence the scores in the tropics.

The shadowing effect is further illustrated in figures 5. The bathymetry for the old operational run (figure 5a) does not represent the Shetlands and Orkney islands and the water depth at the location of the Faeroe islands was reduced but not set to land. When compared to the e-suite configuration (figure 5b), it is obvious that the old operation run does not take into account the local effect of small islands. The new scheme seems to handle the presence of isolated islands by creating a realistic shadow zone which does not extend indefinitely in the lee of the island. Also note the improved wave field representation along the west coast of Ireland as a result of the local bathymetric corrections.

3. RESULTS OF THE PARALLEL RUN

The operational and e-suite wave analysis can be compared with independent buoy observations (see Tech Memo 229 by *Janssen et al.* (1996) or *Janssen et al.* (1997)) for more information on buoy data processing). Please note that this comparison is limited the northern hemisphere, with most buoys in the storm track regions. In any case, the global statistics (figures 6 and 7) indicate a rather neutral effect of the new scheme on the scores. Slight improvements in the wave height statistics are balanced by small deterioration of the peak period statistics. It was discussed how the discrete number of wave energy directional bins does not spread uniformly swell energy. This might results in slightly too much or not enough low frequency energy components at the buoy locations. In that respect the rotation of the spectra is sometime beneficial (improved wave height and peak period) and sometime it is not. This feature is illustrated in figures 8 by looking at buoy time series of wave height and peak period. The wave forecasts can also be compared to the buoy data (tables 1 and 2). No significant difference can really be seen as positive effects are balanced by negative ones.

A more global picture of how the new scheme performed with respect to the operational run is obtained by comparing the wave model first guess with the altimeter wave data. The global picture confirms that few significant differences exist between the two realisations (figures 9, 10, 11). There is, however, a small improvement in the tropics (figure 10) which falls in line with a better north-south advection described earlier.

A similar picture can be drawn from the forecast verification (figures 12). It indicates a minor improvement in the tropics not seen in the other areas (figure 12b).

4. CONCLUSIONS

Even though scores seems to indicate that the rotation of the spectral directional bins by 15 degrees has no significant impact on the global scores of the global wave model, we have shown that it solves the problem of unrealistic wave propagation behind small islands as well as removing the occasional north-south propagation of elongated wave features along meridians. The more consistent advection of wave energy might be responsible for the small positive impact in the tropics. Note however, that the neutral global impact should be attributed to the positive-negative pattern which is brought about by the inherent garden-sprinkler effect of the discrete advection scheme.

With this new scheme, we have brought back the small islands that had been artificially removed from the new operational 0.5 reduced grid. We have also enhanced some islands in the North Sea and redefined a few sea points around Ireland. In this manner, we are making a full use of the improved high resolution and its expected higher spatial and temporal variability.

The first operational analysis produced with this new scheme was carried out for the analysis cycle of the 14th of May 1997, 12Z for both global and mediterranean models.

REFERENCES

Bidlot J., B. Hansen, P. Janssen, 1997: Modification of the ECMWF WAM Code. ECMWF Technical Memorandum 232, ECMWF, Reading.

Booij N., L. Holthuisen, 1987: Propagation of ocean waves in discrete spectral wave models. J. Comput. Phys. 68 307-326.

Janssen P., B. Hansen, J. Bidlot, 1996: Verification of ECMWF wave forecasting system against buoy and altimeter data. ECMWF Technical Memorandum 229, ECMWF, Reading.

Janssen P., B. Hansen, J-R. Bidlot, 1997: Verification of ECMWF wave forecasting system against buoy and altimeter data. to appear in Weather and Forecasting, December 1997.

SWAMP 1985: Sea wave modelling project (SWAMP). An intercomparison study of wind wave prediction models, part 1: principal results and conclusion, in Ocean wave modelling, Plenum, New York, 256 p.

APPENDIX A

The following software changes were necessary to run WAM with the directional bins rotated by half the bin width

The actual directions are defined when PREPROC is run, see subroutine MFREDIR. The necessary change is

```
C
C*     2. COMPUTATION OF DIRECTIONS, BANDWIDTH, SIN AND COS.
C         ------------------------------------------------
C
 2000 CONTINUE
DELTH = ZPI/REAL(KL)
DELTR = DELTH*R
DO 2001 K=1,KL
cccc previously:TH(K) = REAL(K-1)*DELTH
TH(K) = REAL(K-1)*DELTH + 0.5*DELTH
COSTH(K) = COS(TH(K))
SINTH(K) = SIN(TH(K))
2001 CONTINUE
```

Few changes were necessary to accomodate the new definition for the initial direction which was previously defined in a parameter statement as 0.(variable TH0) without any connection with the value defined in MFREDIR which is available as the first value of array TH (common block FREDIR). TH(1) is now passed to subroutine HEADBC which should read :

```
SUBROUTINE HEADBC (NBOUNC, IDELPRO, TH0, FR1, IU19, IU06)
C ----------------------------------------------------------------
C
C**** *HEADBC* - OUTPUT OF THE COARSE GRID BOUNDARY VALUE FILE HEADER.
C
C R. PORTZ   MPI        JANUARY 1991
C J. BIDLOT  ECMWF      JANUARY 1997  : TH0 IS PASSED AS AN ARGUMENT
C
C* PURPOSE.
C  --------
C
C WRITE A HEADER TO THE BOUNDARY VALUE OUTPUT FILE.
C
C** INTERFACE.
C   ----------
C
C  *CALL* *HEADBC (NBOUNC, IDELPRO, TH0, FR1, IU19, IU06)*
C  *NBOUNC*   - NUMBER OF OUTPUT POINTS.
C  *IDELPRO* - PROPAGATION = OUTPUT TIMESTEP (SECONDS).
C  *TH0*      - FIRST DIRECTION (IN RADIAN)
C  *FR1*      - FIRST FREQUENCY (HERTZ).
C  *IU19*     - OUTPUT UNIT OF BOUNDARY VALUES.
C  *IU06*     - PRINTER OUTPUT UNIT.
```

```
C
C METHOD.
C -------
C
C  SEQUENTIAL UNFORMATED WRITE TO UNIT.
C
C EXTERNALS.
C ----------
C
C  *ABORT1*     - TERMINATES PROCESSING.
C
C REFERENCE.
C ----------
C
C NONE.
C
C ------------------------------------------------------------------
C
#include "param.h"
C
C ------------------------------------------------------------------
C
PARAMETER (CO = 1.1)
C
C* VARIABLE.    TYPE.      PURPOSE.
C  ---------    ------     --------
C  *CO*         REAL       FREQUENCY RATIO.
C
C ------------------------------------------------------------------
C
C*1. FORMAT AND WRITE HEADER.
C  --------------------------
C
1000 CONTINUE
   XANG = REAL(NANG)
   XFRE = REAL(NFRE)
   XBOU = REAL(NBOUNC)
   XDEL = REAL(IDELPRO)
   WRITE(IU19,ERR=2000) XANG, XFRE, TH0, FR1, CO, XBOU, XDEL

   RETURN
C
C ------------------------------------------------------------------
C
C*2. ERROR MESSAGE.
C     --------------
C
```

```
2000 CONTINUE
   WRITE(IU06,*) '*******************************************'
   WRITE(IU06,*) '*                                         *'
   WRITE(IU06,*) '*    FATAL ERROR IN SUB. HEADBC           *'
   WRITE(IU06,*) '*    ==========================           *'
   WRITE(IU06,*) '*                                         *'
   WRITE(IU06,*) '*    WRITE ERROR FROM UNIT:IU19 = ',IU19  *'
   WRITE(IU06,*) '*                                         *'
   WRITE(IU06,*) '*    PROGRAM ABORTS                       *'
   WRITE(IU06,*) '******************************************'
   CALL ABORT1
END
```

Since there is an extra argument to HEADBC, the call to it must be modified in INITMDL (at the end of it) :

```
CNEST
C
CWRITE BOUNDARY VALUE FILE HEADER.
C
   IF (IBOUNC.EQ.1) THEN
      CALL HEADBC (NBOUNC, IDELPRO, TH(1), FR(1), IU19, IU06)
   IF (ITEST.GE.2)
1     WRITE(IU06,'(''     SUB. INITMDL: HEADER FOR  '',
2     ''COARSE GRID WAS WRITTEN OF UNIT IU19 = '',A8)') IU19
ENDIF
CNEST
```

and in WAMODEL (before 1.8.3)

```
CNEST
C
C SAVE BOUNDARY VALUE FILE.
C
   IF (IBOUNC.EQ.1) THEN
      CALL GSFILE (IU06, IU19, 0, CDTPRO, CDATEF, 'CBO', 'S')
   IF (CDTPRO.LT.CDATEE)
1     CALL HEADBC (NBOUNC, IDELPRO, TH(1), FR(1), IU19, IU06)
ENDIF
CNEST
```

The same problem exists in OUTSPP where TH0 was defined in a parameter statement without any link to TH(1). It was corrected by explictly linking TH0 to TH(1). The following 3 corrections are needed:

1. Remove TH0 from parameter statement:

```
C
ccc previouslyPARAMETER (TH0 = 0., CO = 1.1)PARAMETER ( CO = 1.1)
C
C*VARIABLE.  TYPE.     PURPOSE.
C ---------  -------   --------
C *CO*       REAL      FREQUENCY RATIO.
C
```

2. Add definition of TH0:

```
C
C* 1.1.1 FILE OUTPUT TO IU25.
C       --------------------
C
   IF (FFLAG(17)) THEN
      XANG = REAL(NANG)
      XFRE = REAL(NFRE)

cccc insert next line
   TH0 = TH(1)*DEG
cccc

   WRITE(IU25) XLON, XLAT, CDTPRO, XANG, XFRE,
1        TH0, FR(1), CO
      WRITE(IU25) 4.*SQRT(EMEAN(IJ)), DEG*THQ(IJ),
1        FMEAN(IJ), US(IJ), DEG*THW(IJ),
2        U10(IJ)
      IF(LMESSPASS) THEN
         WRITE(IU25) ((FLPTS(1,NGOU,K,M),K=1,NANG),M=1,NFRE)
      ELSE
         WRITE(IU25) ((FL3(IJ,K,M),K=1,NANG),M=1,NFRE)
   ENDIF
ENDIF
```

3. Add definition of TH0:

```
C
C* 1.2.1FILE OUTPUT TO IU26.
C       --------------------
C
   IF (FFLAG(18)) THEN
      XANG = REAL(NANG)
      XFRE = REAL(NFRE)

cccc insert next line
      TH0 = TH(1)*DEG
cccc

      WRITE(IU26) XLON, XLAT, CDTPRO, XANG, XFRE,
1        TH0, FR(1), CO
      WRITE(IU26) EWSEA, 4.*SQRT(ESWELL(IJ)),
1        DEG*THWISEA(IJ), DEG*THSWELL(IJ),
2        FWSEA, FSWELL(IJ)
      WRITE(IU26) ((SPEC(K,M),K=1,NANG),M=1,NFRE)
   ENDIF
C
```

The same problem exists in OUTERS where TH0 was defined in a parameter statement without any link to TH(1). It was corrected by explictly replacing TH0 by TH(1). The following 2 corrections are needed:

1. remove TH0 from parameter statement:

```
C
cccc previously PARAMETER (TH0 = 0., FREI = 1.1)
PARAMETER ( FREI = 1.1)
C
C FREI   REAL  FREQUENCY INCREMENT
C
```

2. replace TH0 by TH(1) in the write statement

```
* 1.1 WRITE INFORMATION TO FILE IU92.
C     ------------------------------
C
      WRITE(IU92) XLON, XLAT, CDTPRO, XANG, XFRE,
   1       TH(1), FR(1), FREI
        WRITE(IU92) 4.*SQRT(EMEAN(IJ)), DEG*THQ(IJ),
   1       FMEAN(IJ), US(IJ), DEG*THW(IJ),
   2       U10(IJ)
```

In case of data assimilation, FWSEA is called to determine the contribution from the windsea to the total spectrum. The difference between wind direction and wave direction is computed. It was computed with the assumption that the first wave direction was pointing north (0 degree) which should not be the case in general. FWSEA was modified to take that into account when computing the parameter IDW:

1.

```
C 2.3 SEARCH A PEAK OF THE SPECTRUM AROUND THE WIND DIRECTION.
C     -------------------------------------------------------
C
THEWI = THMO(IJ)
cccc previously IDW = NINT(THEWI/DELTH)+1
IDW = NINT(MOD(THEWI-TH(1),ZPI)/DELTH)+1
FSMAX = 0.
```

2.

```
C
C*2.4.5 AROUND THE WIND SEA PEAK THE WHOLE MODEL SPECTRUM IS
C*      ASSUMED TO BE WINDSEA.
C       ----------------------------------------------------
C
cccc previously IDW = NINT(THE/DELTH)+1
   IDW = NINT(MOD(THE-TH(1),ZPI)/DELTH)+1
   DO 2451 II=IDW-2,IDW+2
```

The spectra that will be produced with this new version will then be defined with respect to those new directions and should be read as such once PREPROC has been rerun with the modification to MFREDIR to produce a new grid definition file. The rest should follow through. If you output spectra at given output points (OUTSPP) be aware that the first direction is not zero.

APPENDIX B

Corrections to the bathymetry:

With this new definition for the spectral directions, it was found that the islands that had been removed (Hawaii, Solomon, Galapagos, Chatham, Sakalin, Natuna Besar, Mascarene, Kerguelen, South Georgia) could be put back as land.

Few more corrections were added:

Islands added: Hawaiian Islands (Kauai, Oahu, Molokai, Maui)

Hawaii (extra land points)
the Kaiwi channel was set to 100m depth
Great Bahamas
Corrections to some of the Caribbean Is. (Jamaica, Hispaniola)
Shetlands, Orkney, Faeroe and Lewis (Outer Hebrides) islands

Coast lines corrections:

corrected to become sea points with an appropriate water depth:

the west and north-west coastline of Ireland
Scottish coast off Northern Ireland
Welsh central coastline (Cardigan bay)
the Great lakes: Lake Michigan and Lakes Huron.

TABLES

Table 1: Wave height RMSE (m).

Hs	t+0		t+24		t+48		t+72		t+96		t+120	
	ops	e-suite	ops	e-suite	ops	e-suite	ops	e-suite	ops	e-suite	ops	e-suite
all	0.51	0.50	0.56	0.55	0.63	0.62	0.70	0.69	0.81	0.81	0.97	0.96
Hawaii	0.50	0.50	0.52	0.50	0.49	0.46	0.52	0.48	0.55	0.50	0.72	0.67
Japan	0.55	0.53	0.57	0.55	0.70	0.68	0.72	0.71	0.83	0.84	1.09	1.08
NPC	0.79	0.78	0.85	0.83	0.96	0.94	1.07	1.05	1.11	1.12	1.43	1.40
USWC	0.43	0.43	0.54	0.54	0.62	0.61	0.74	0.74	1.08	1.10	0.92	0.92
USEC	0.51	0.50	0.53	0.53	0.58	0.58	0.57	0.57	0.78	0.78	0.85	0.85
CANEC	0.88	0.87	0.94	0.93	0.97	0.96	1.06	1.02	1.04	1.05	1.33	1.38
GM	0.34	0.34	0.46	0.45	0.58	0.57	0.55	0.52	0.66	0.65	0.84	0.82
NEATL	0.45	0.44	0.50	0.50	0.57	0.56	0.65	0.64	0.78	0.78	0.91	0.91
NSea	0.32	0.30	0.50	0.50	0.57	0.56	0.65	0.64	0.78	0.78	0.91	0.91
Channel	0.41	0.38	0.42	0.41	0.51	0.51	0.54	0.52	0.57	0.54	0.74	0.73

Wave height root mean square errors as a function of forecast day from December 5, 1996 to January 17, 1997. The statistics were obtained from the comparison of the model results with 6-hourly averaged moored buoy data. The RMSE are given for all 40 buoys and as well as for regions: Hawaii (51001, 51002, 51003, 51004), Japan (21004, 22001), the North PacifiC area (46001, 46003, 46035, 46184), off-shore from the US West Coast (46002, 46005, 46006, 46025, 46036, 46059), off-shore from the US East Coast (41001, 41002, 41010, 44008, 44011), the Canadian East Coast (44137, 44138, 44141), the Gulf of Mexico (42001), the North East Atlantic (62029, 62081, 62105, 62106, 62163, 64045), the North SEA (62026, 62109, 62112, 62165, 63111) and the English Channel area (62103, 62107, 62303, 62305).

Table 2: Peak period RMSE (sec.)

Tp	t+0		t+24		t+48		t+72		t+96		t+120	
	ops	e-suite	ops	e-suite	ops	e-suite	ops	e-suite	ops	e-suite	ops	e-suite
all	1.81	1.83	1.89	1.87	1.97	1.91	2.21	2.09	2.31	2.31	2.42	2.34
Hawaii	1.60	1.76	1.67	1.66	1.79	1.70	2.08	1.85	2.40	2.24	2.66	2.55
Japan	2.59	2.48	2.58	2.52	2.63	2.70	3.08	3.02	2.62	2.81	2.96	2.90
NPC	1.79	1.76	1.84	1.87	1.93	1.99	2.21	2.18	2.12	2.17	2.20	2.20
USWC	1.45	1.50	1.42	1.50	1.62	1.65	1.81	1.70	2.20	2.12	2.00	2.02
USEC	1.86	2.07	2.25	2.20	2.25	2.18	2.33	2.10	2.59	2.61	2.59	2.46
CANEC	1.51	1.30	1.58	1.37	1.53	1.32	1.69	1.59	1.55	1.37	1.96	1.72
GM	1.64	1.84	1.24	1.40	1.11	1.14	1.22	1.29	1.26	1.34	1.37	1.45

Same as table 1 but for wave peak period. Note that the UKMO buoys do not report peak period.

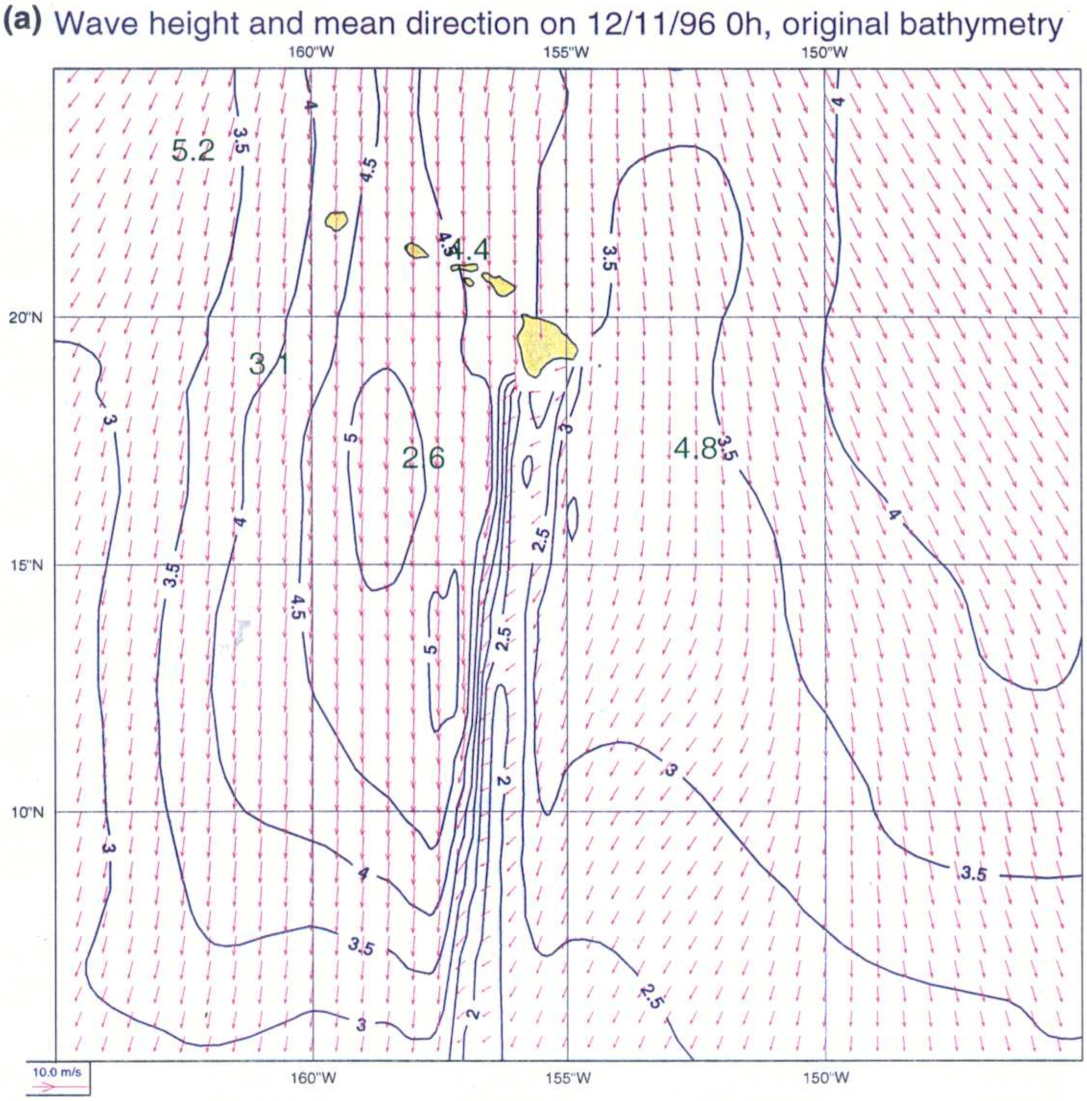

Fig. 1 Analysed wave height (0.5 m contours) and mean wave direction (10m arrow length) around the Hawaiian Islands. On November 12, 1996, a wave system had been propagating from the North to the South, before interacting with the localised islands. The large (green) numbers are the corresponding synoptic wave height observations from the NDBC network. (a) In the original high resolution bathymetry, only Hawaii is present. Since the discretised spectral bin directions coincide in part with the coordinate axis directions, an unrealistic shadow appears in the lee of Hawaii.

(b) wave height and mean direction on 12/11/96 0h, operational settings : islands removed

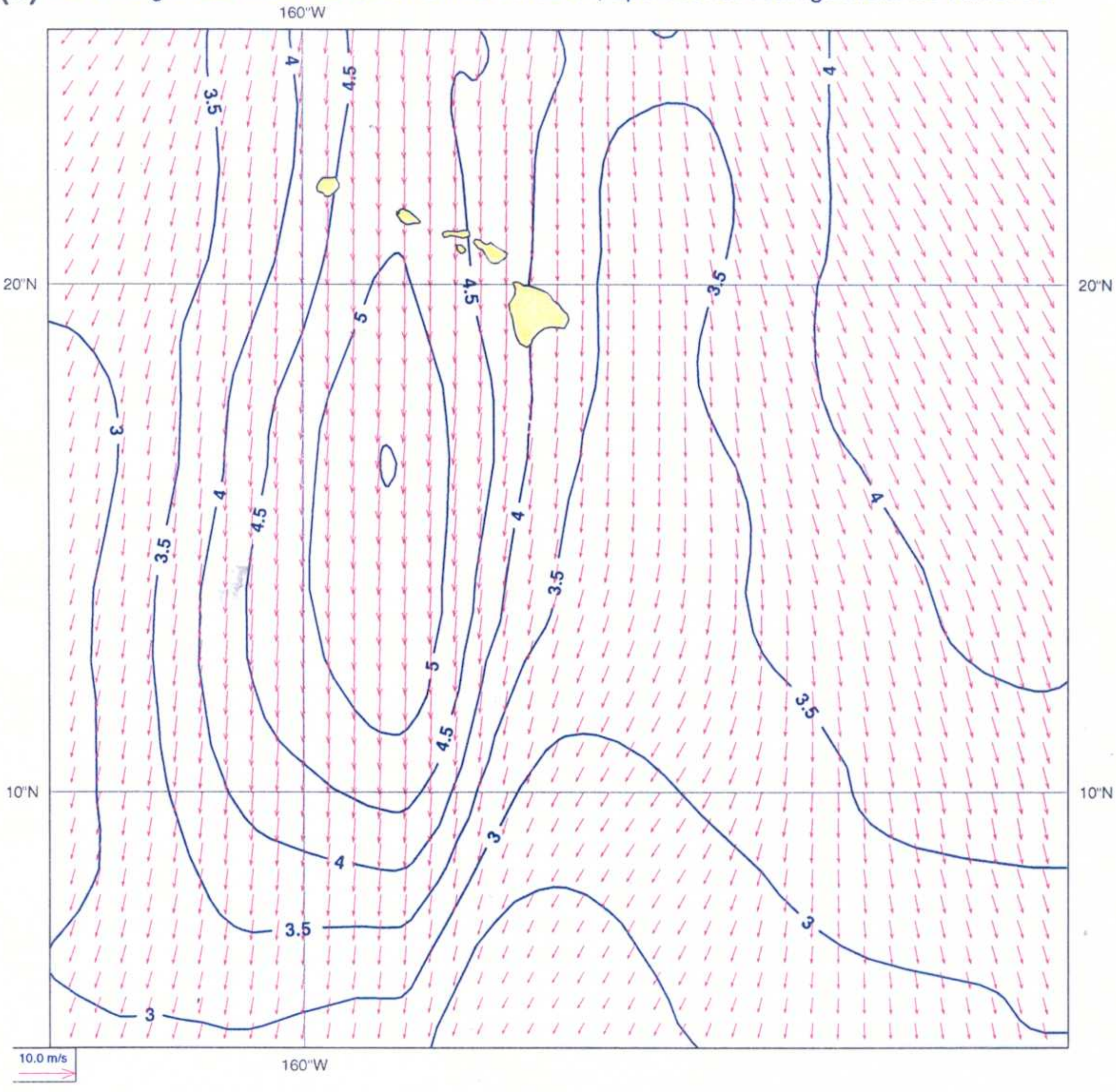

Fig. 1 (b) In the old operational high resolution settings (5th December 1996 to 13th May 1997), Hawaii was removed in order to alleviate the shadow problem.

(c) Wave height and mean direction on 12/11/96 0h, rotated spectra and added islands

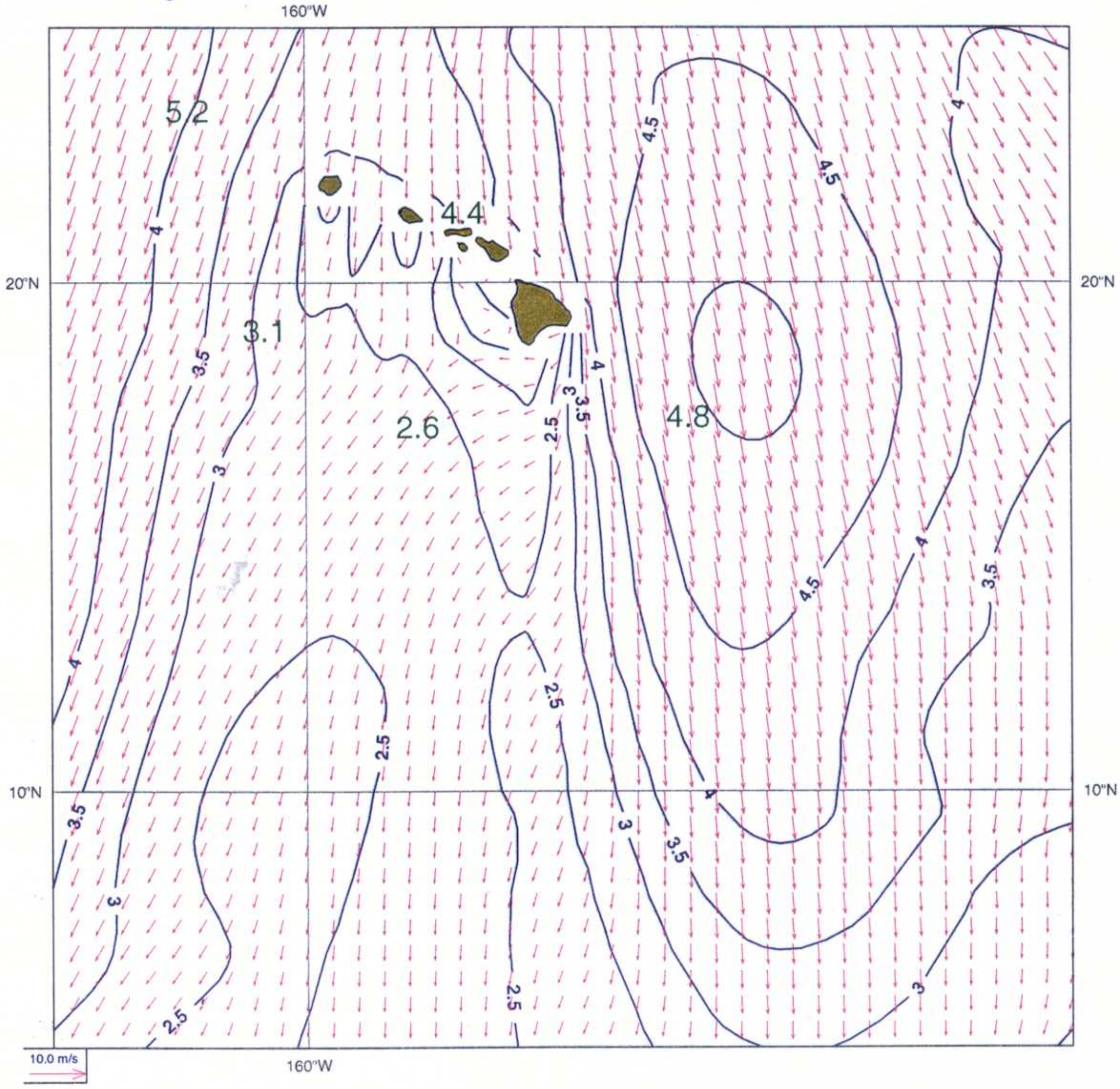

Fig. 1 (c) By rotating the spectral bin directions by 15°, a more realistic North-South propagation was obtained. The main Hawaiian Islands were reintroduced, resulting in a more realistic shadow in the lee of the islands

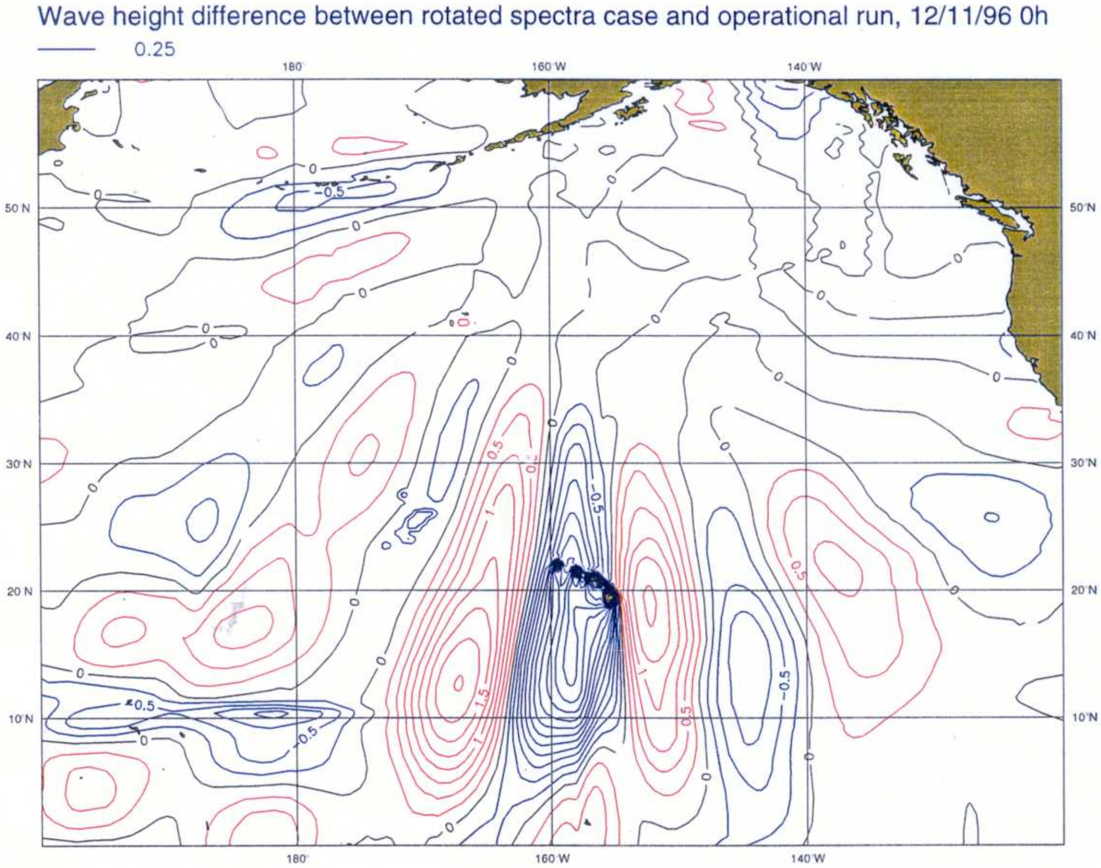

Fig. 2 Analysed wave height difference between the case of figure 1c and figure 1b. 0.25m contour lines are used. Red solid contours denote positive differences and blue dashed negative ones. The difference in directional discretisation clearly resulted in an uneven distribution of swell wave energy. This effect is also know was the garden sprinkler effect.

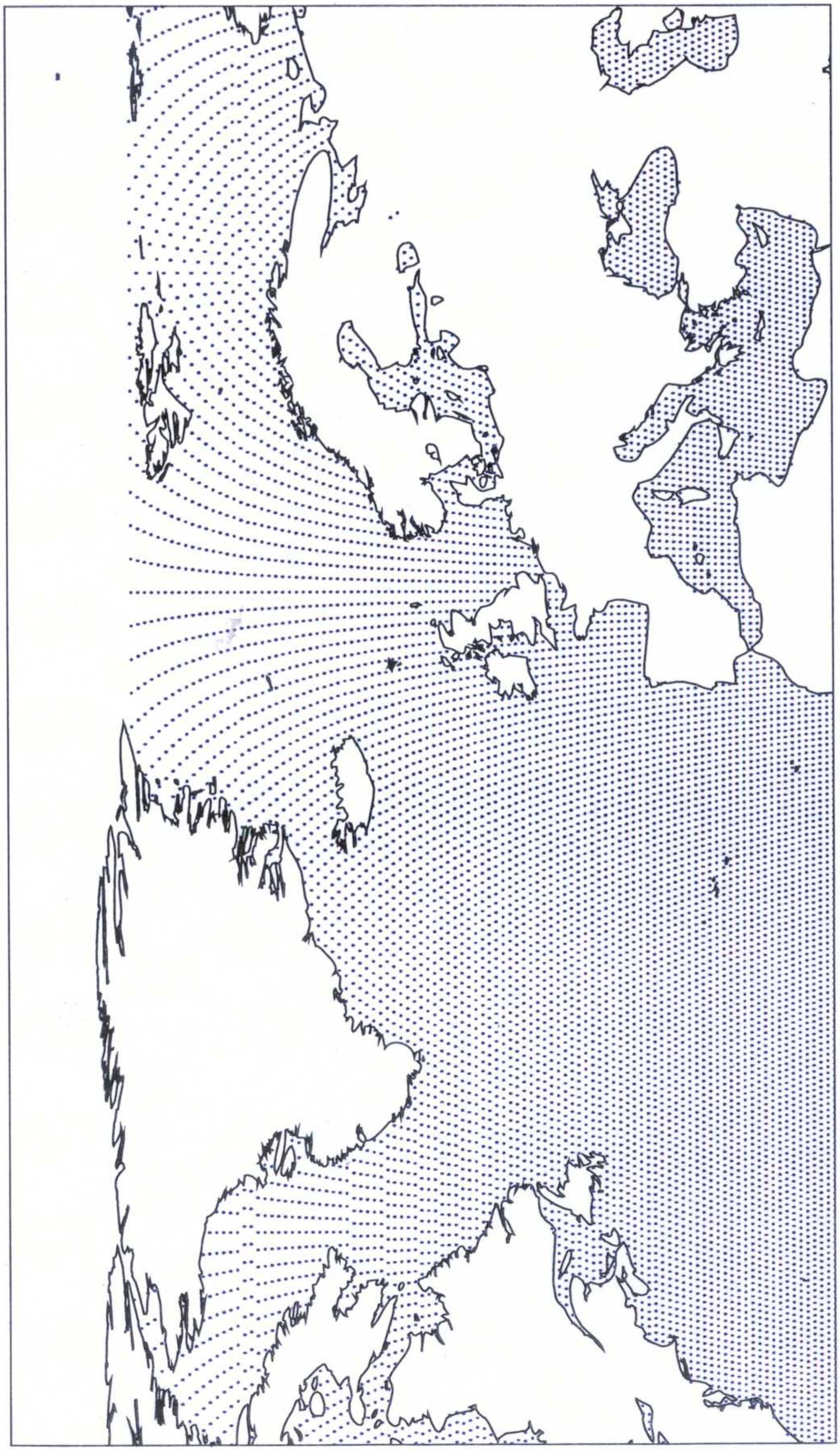

Fig. 3 New 0.5° reduced latitude-longitude grid used by the ECMWF operational wave model from May 14, 1997, 12Z.

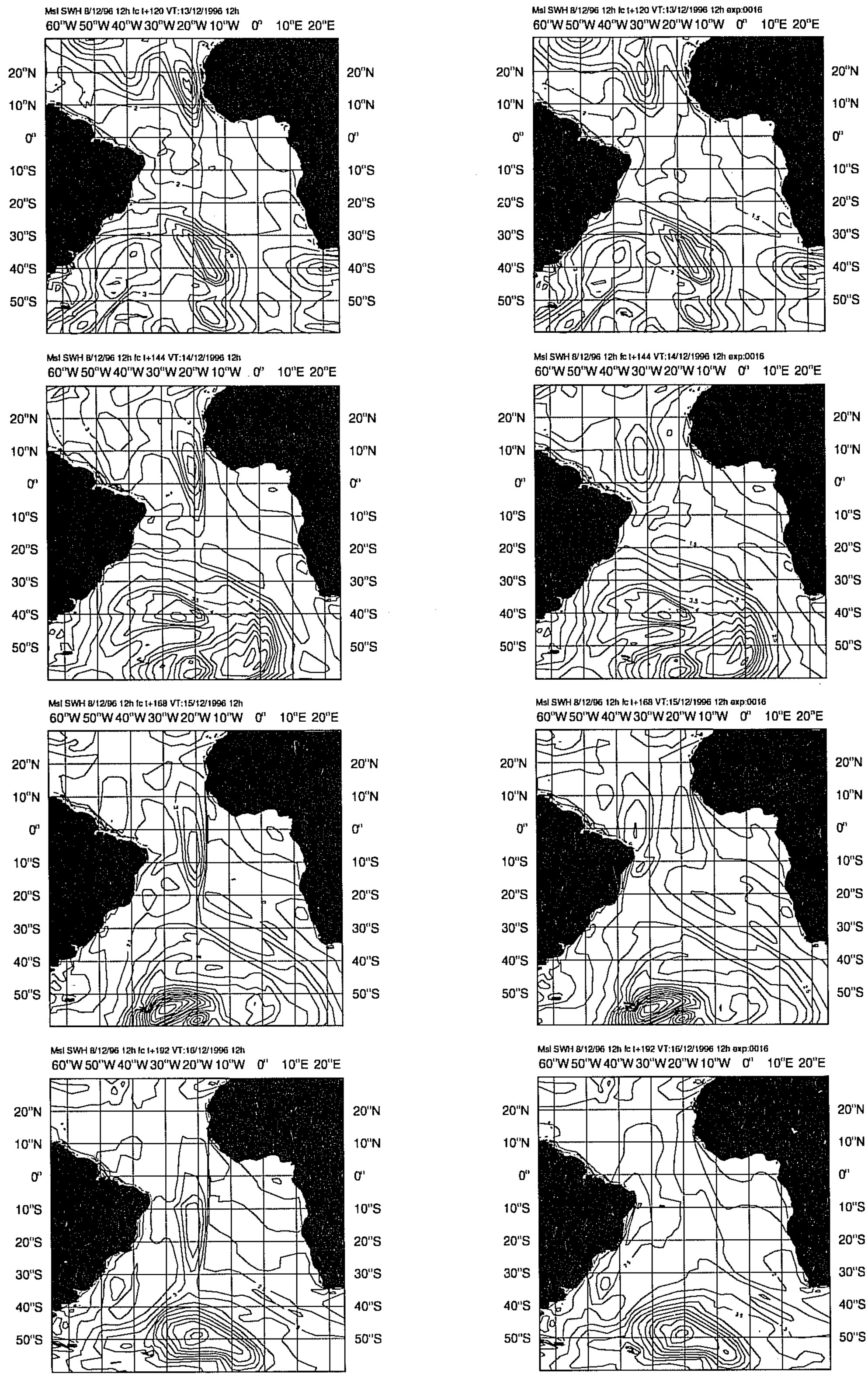

Fig. 4 Wave height forecast (day 5-8 from 8/12/96) for the old operational (left panels) and the rotated spectra experiment (e-suite 0016) (right panels). 0.5m contours are used. Note the elongated feature propagating southward in the operational run which is not present (a lot more diffused) in the e-suite.

(a)

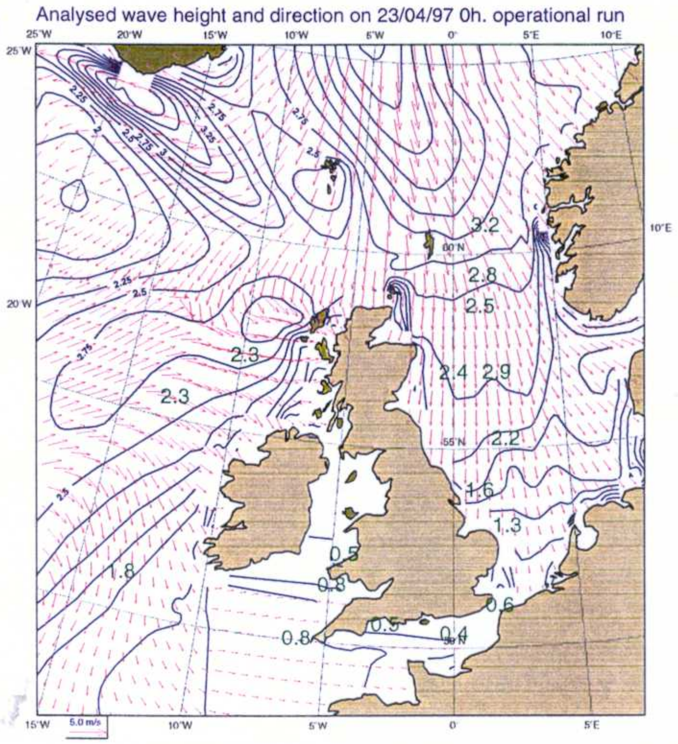

(b)

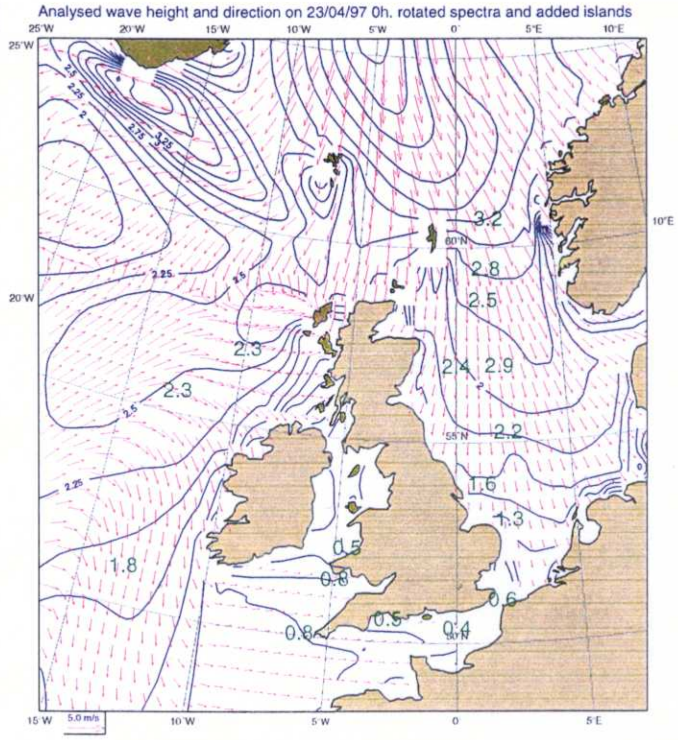

Fig. 5 Analysed wave height (0.25m contours) on April 23, 1997, 0h around the British Islands. The synoptic wave observations as obtained from the global telecommunication system are also shown (large green numbers). (a) the (old) operational run (b) the e-suite experiment (future operational) for which the spectral bin direction were rotated by 15° and a few bathymetric corrections were applied to better represent the North Sea islands and the western coast of Ireland.

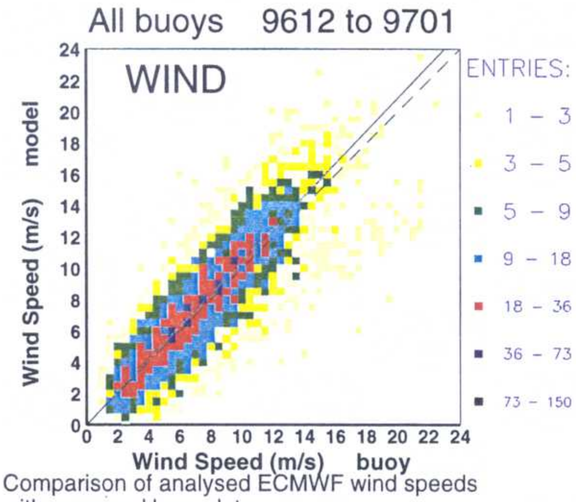

Comparison of analysed ECMWF wind speeds with averaged buoy data.

21004 46003 62081
22001 46005 62103
41001 46025 62105
41002 46035 62106
41010 46036 62109
42001 46059 62112
44008 46184 62163
44011 51001 62165
44137 51002 62303
44138 51003 62305
44141 51004 63111
46001 62026 64045
46002 62029

ENTRIES = 4842
MODEL MEAN = 8.094 STDEV = 3.834
BUOY MEAN = 7.830 STDEV = 3.520
LSQ FIT: SLOPE = 0.930 INTR = 0.816
RMSE = 2.030 BIAS = 0.265
CORR COEF = 0.853 SI = 0.257
SYMMETRIC SLOPE = 1.043

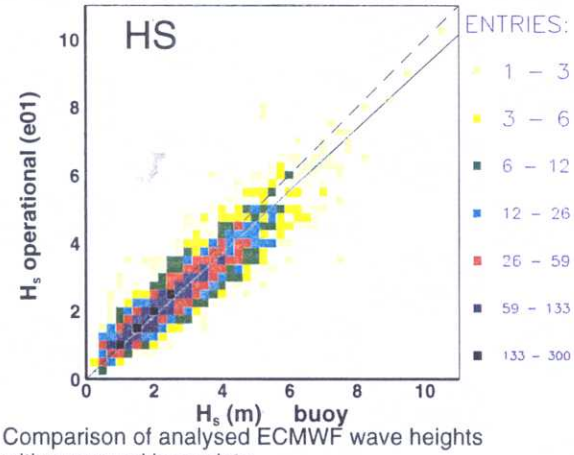

Comparison of analysed ECMWF wave heights with averaged buoy data.

21004 46003 62029 64045
22001 46005 62081
41001 46006 62103
41002 46025 62105
41010 46035 62106
42001 46036 62107
44008 46059 62109
44011 46184 62112
44137 51001 62163
44138 51002 62165
44141 51003 62303
46001 51004 62305
46002 62026 63111

ENTRIES = 5681
MODEL MEAN = 2.434 STDEV = 1.153
BUOY MEAN = 2.598 STDEV = 1.334
LSQ FIT: SLOPE = 0.809 INTR = 0.332
RMSE = 0.505 BIAS = -0.164
CORR COEF = 0.937 SI = 0.184
SYMMETRIC SLOPE = 0.922

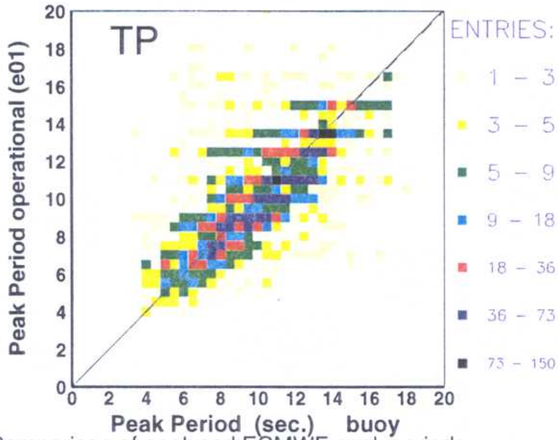

Comparison of analysed ECMWF peak periods with averaged buoy data.

21004 46003
22001 46005
41001 46006
41002 46025
41010 46035
42001 46036
44008 46059
44011 46184
44137 51001
44138 51002
44141 51003
46001 51004
46002

ENTRIES = 3326
MODEL MEAN = 10.281 STDEV = 2.584
BUOY MEAN = 10.212 STDEV = 2.703
LSQ FIT: SLOPE = 0.722 INTR = 2.913
RMSE = 1.856 BIAS = 0.070
CORR COEF = 0.755 SI = 0.182
SYMMETRIC SLOPE = 1.004

Fig. 6 Comparison of the operational analysed ECMWF 10m wind speed, wave height, and peak period with buoy observations form December 5, 1996 to January 17, 1997. The list of the buoys used is presented to the right of the scatter plots. The buoy data were averaged in 6 hour time windows centred around synoptic times following a basic quality check (Janssen et al, 1996)

All buoys 9612 to 9701

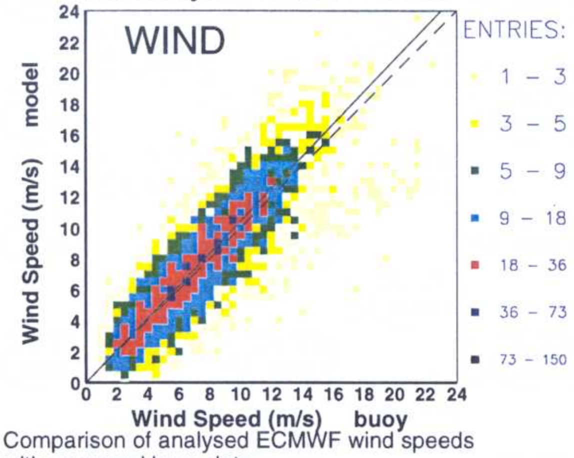

21004 46003 62081
22001 46005 62103
41001 46025 62105
41002 46035 62106
41010 46036 62109
42001 46059 62112
44008 46184 62163
44011 51001 62165
44137 51002 62303
44138 51003 62305
44141 51004 63111
46001 62026 64045
46002 62029

ENTRIES = 4842
MODEL MEAN = 8.094 STDEV = 3.834
BUOY MEAN = 7.830 STDEV = 3.520
LSQ FIT: SLOPE = 0.930 INTR = 0.816
RMSE = 2.031 BIAS = 0.265
CORR COEF = 0.853 SI = 0.257
SYMMETRIC SLOPE = 1.043

Comparison of analysed ECMWF wind speeds with averaged buoy data.

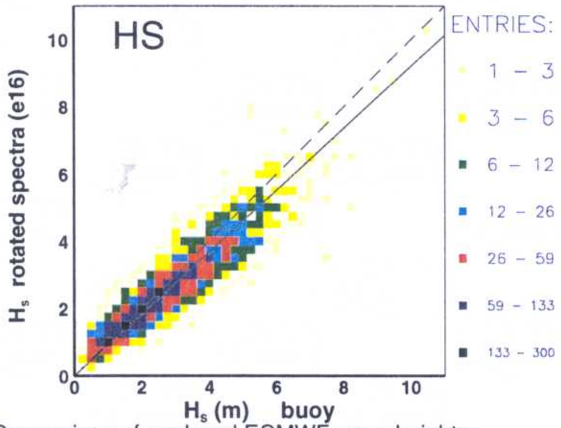

21004 46003 62029 64045
22001 46005 62081
41001 46006 62103
41002 46025 62105
41010 46035 62106
42001 46036 62107
44008 46059 62109
44011 46184 62112
44137 51001 62163
44138 51002 62165
44141 51003 62303
46001 51004 62305
46002 62026 63111

ENTRIES = 5681
MODEL MEAN = 2.431 STDEV = 1.140
BUOY MEAN = 2.598 STDEV = 1.334
LSQ FIT: SLOPE = 0.803 INTR = 0.344
RMSE = 0.498 BIAS = -0.167
CORR COEF = 0.940 SI = 0.181
SYMMETRIC SLOPE = 0.919

Comparison of analysed ECMWF wave heights with averaged buoy data.

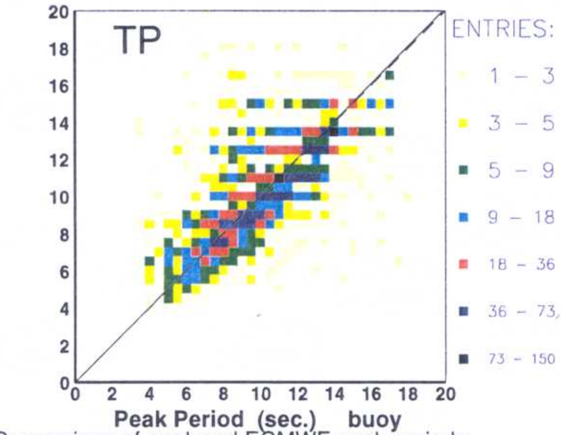

21004 46003
22001 46005
41001 46006
41002 46025
41010 46035
42001 46036
44008 46059
44011 46184
44137 51001
44138 51002
44141 51003
46001 51004
46002

ENTRIES = 3326
MODEL MEAN = 10.311 STDEV = 2.594
BUOY MEAN = 10.212 STDEV = 2.702
LSQ FIT: SLOPE = 0.718 INTR = 2.978
RMSE = 1.885 BIAS = 0.099
CORR COEF = 0.748 SI = 0.184
SYMMETRIC SLOPE = 1.007

Comparison of analysed ECMWF peak periods with averaged buoy data.

Fig. 7 Same as figure 6 but for the e-suite experiment for which the spectral bin direction were rotated by 15°

(a)

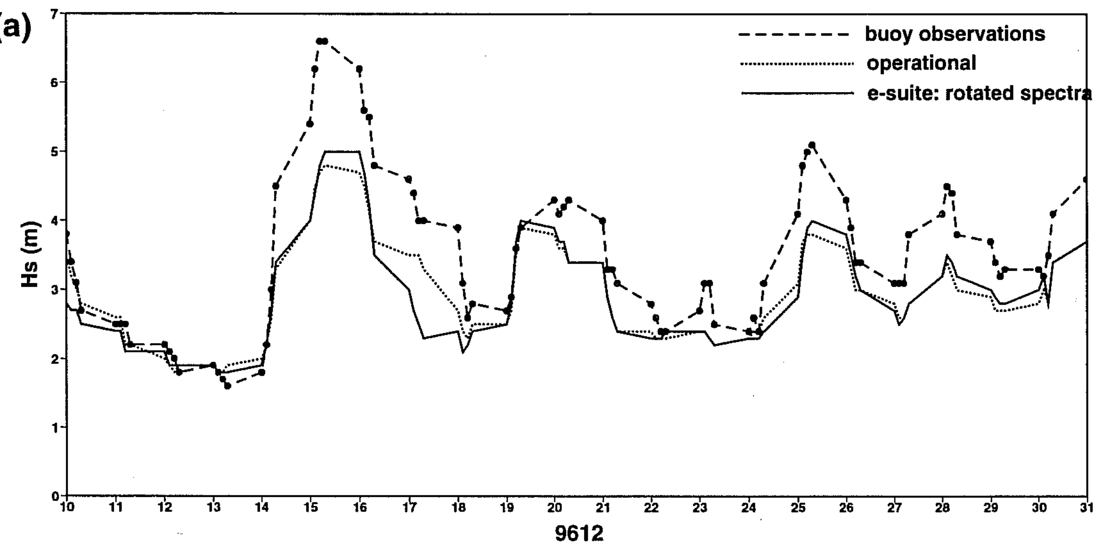

(b)

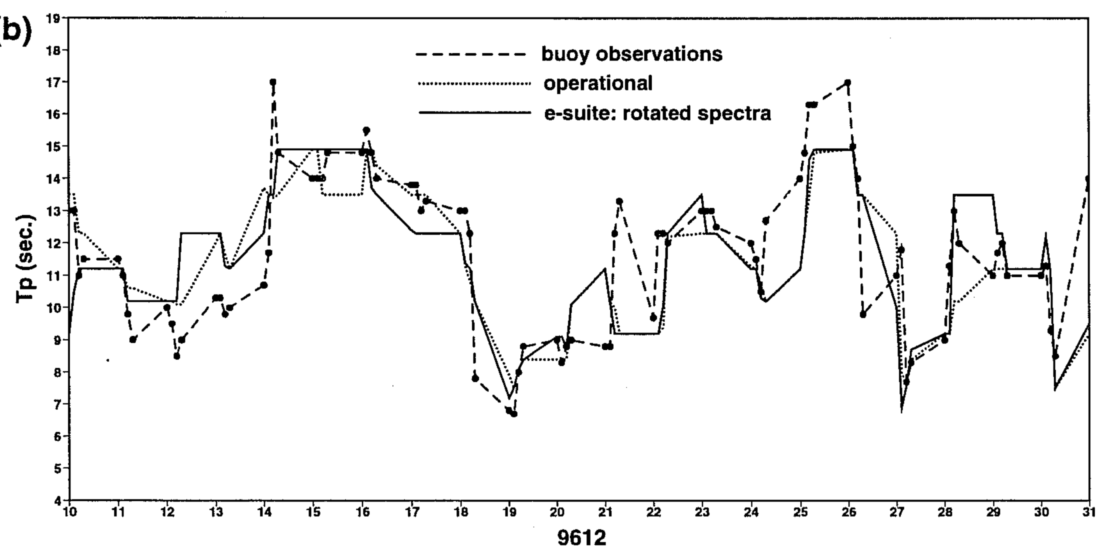

Fig. 8 Time series of buoy observations and model output. Buoy data were averaged in 6 hour time windows after a basic quality check. Model data were interpolated to the buoy locations. (a) Wave height at 51001 (23.4°N, 162.3°W, North West Hawaii) (b) Wave peak period at 51001 (23.4°N, 162.3°W, North West Hawaii)

(c)

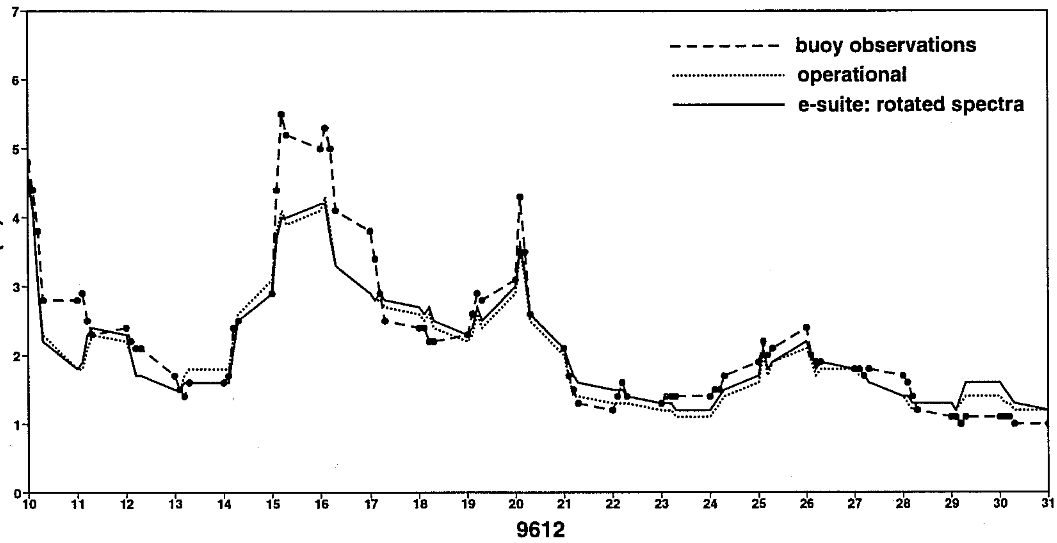

(d)

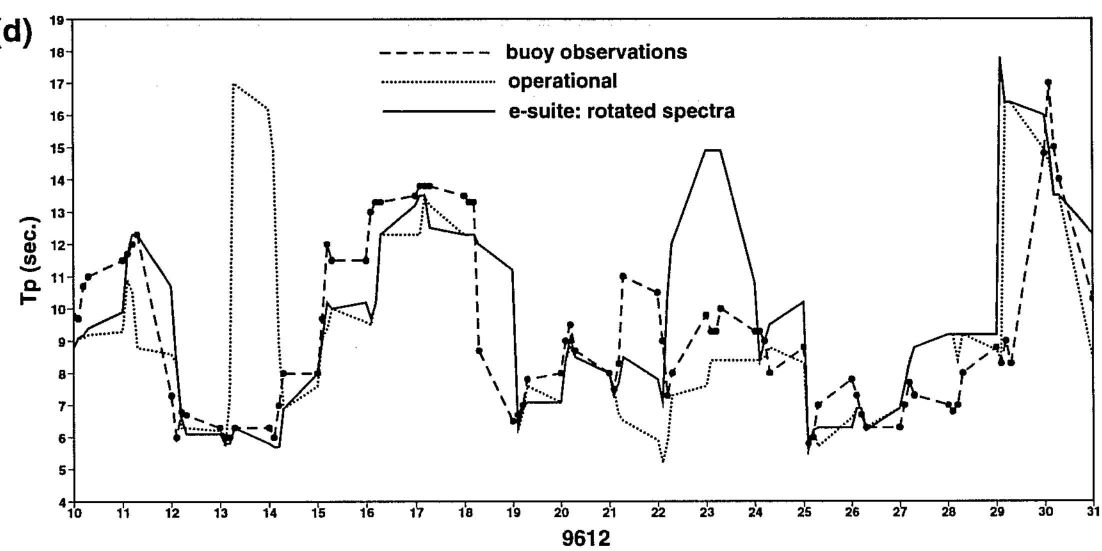

Fig. 8 (c) Wave height at 41002 (32.3°N, 75.2°W, South Hatteras) (d) Wave peak period at 41002 (32.3°N, 75.2°W, South Hatteras)

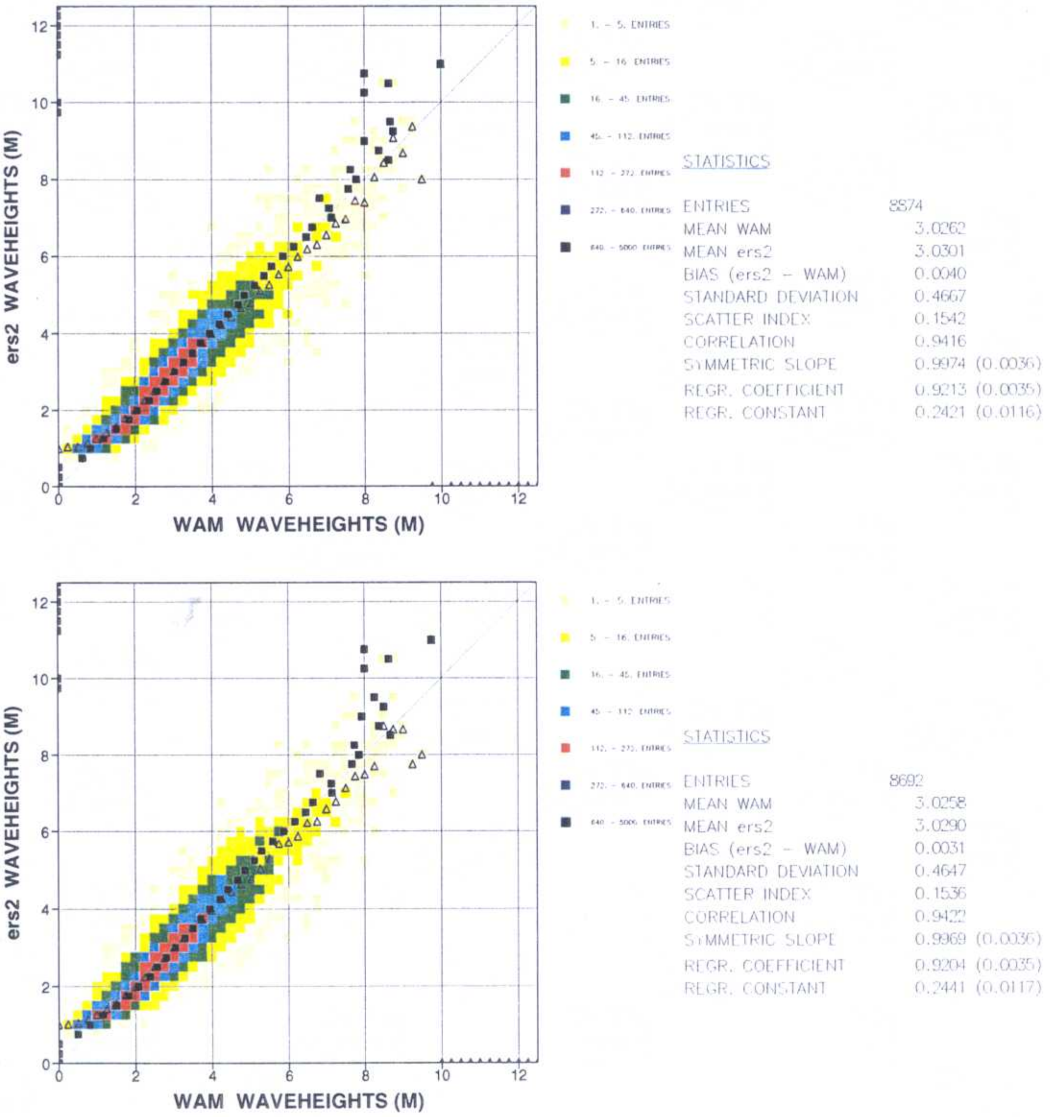

Fig. 9 Scatter diagrams for wave heights in the northern hemisphere for December 1996. ERS-2 altimeter wave data are compared with the wave model first guess. Satellite super observations are created by averaging 30 along track single observations that passed an extensive quality control procedure. The model data are interpolated both in space and time to the location of the satellite super observations. (a) the (old) operational run. (b) the e-suite experiment (future operational) for which the spectral bin direction were rotated by 15°.

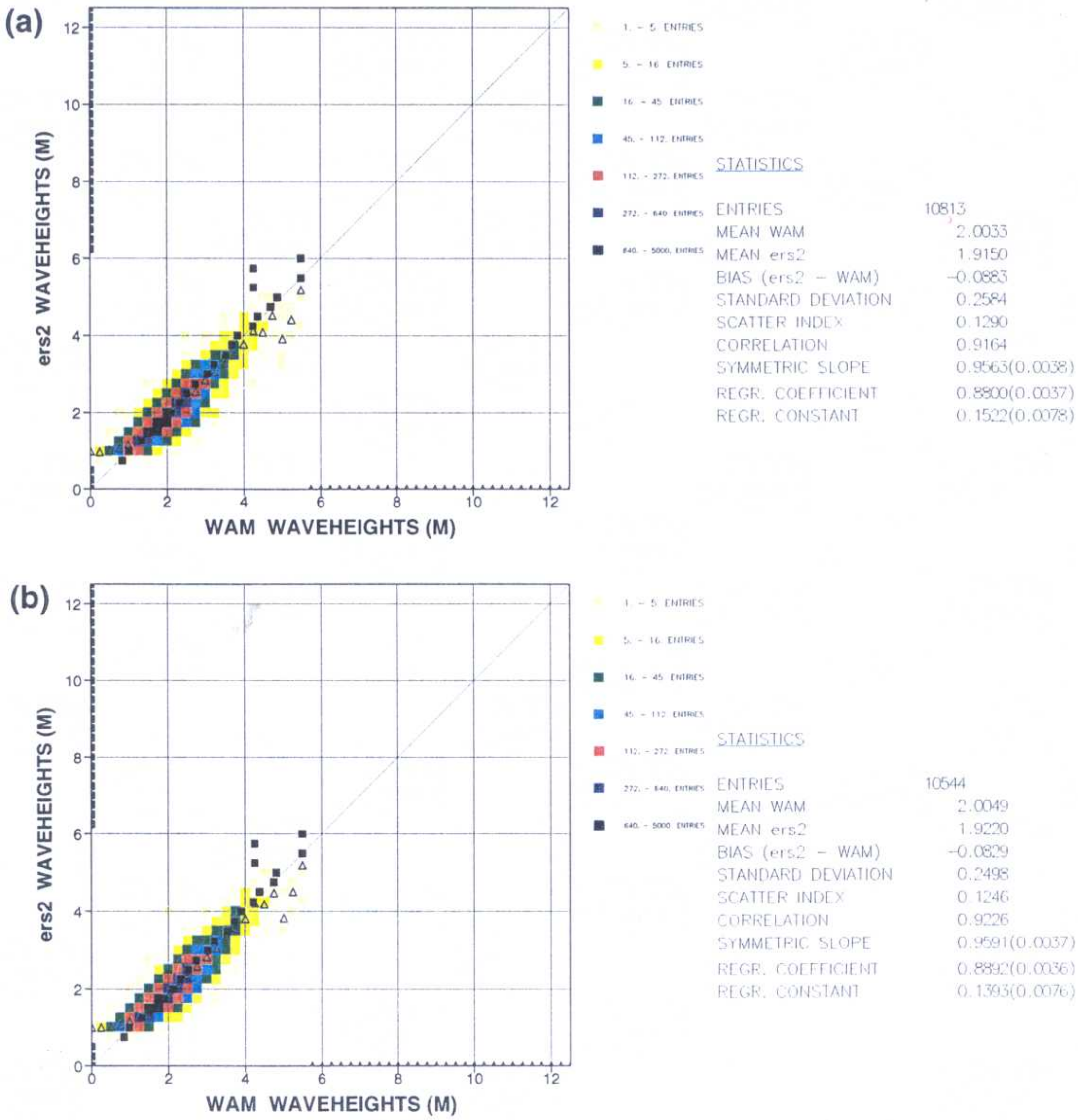

Fig. 10 Same as figure 9 but for the tropics

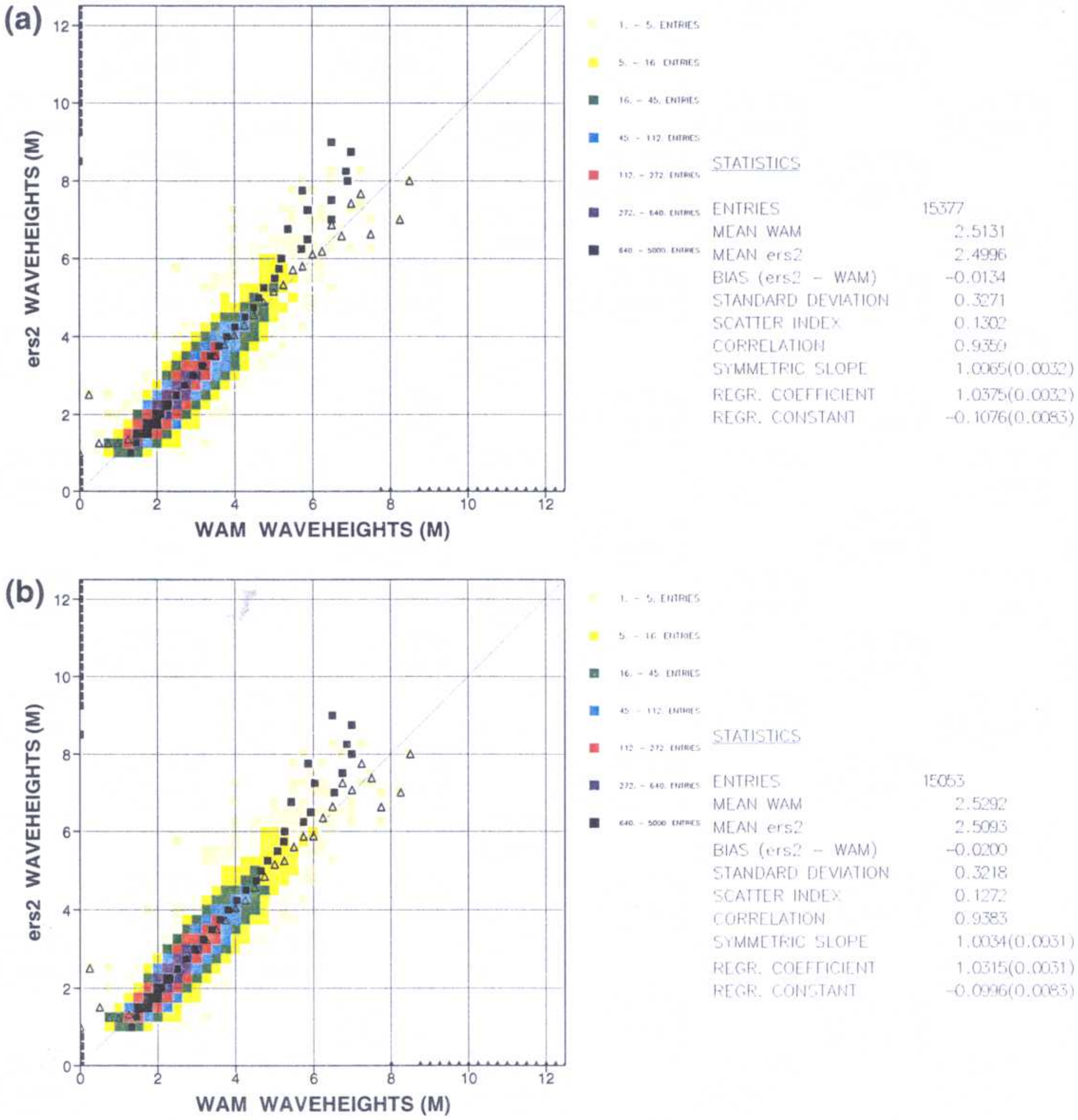

Fig. 11 Same as figure 9 but for the southern hemisphere.

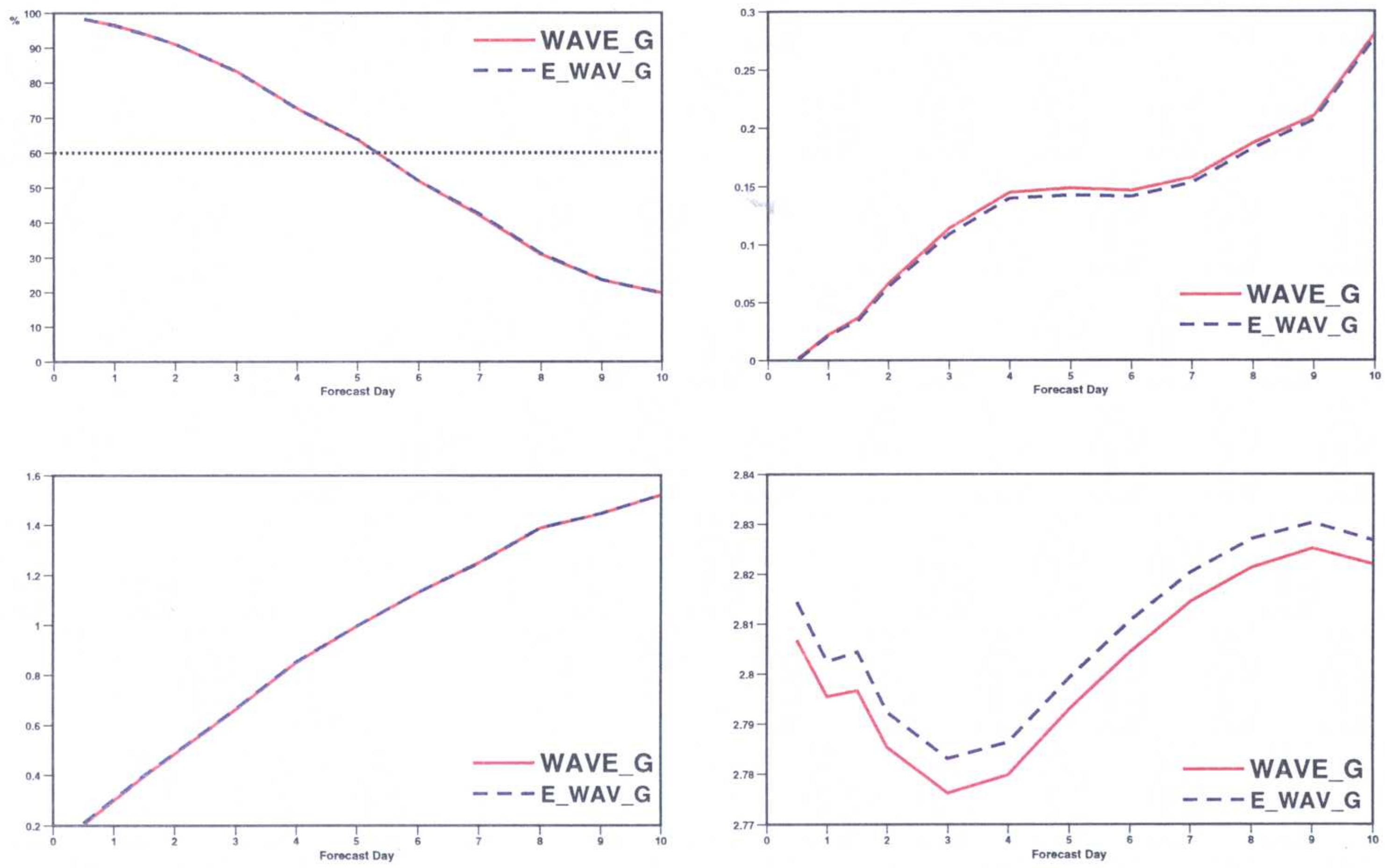

Fig. 12 Forecast verification scores based on the respective verifying wave analysis for December 1996 between the operational run (solid line: WAVE_G) and the e-suite (dashed line: E_WAV_G). The upper left panel shows the anomaly correlation of the forecast. The mean error is displayed in the upper right panel and the standard deviation of error in the lower left panel. The mean of the respective verifying analysis is plotted in the lower right panel. (a) scores for the northern hemisphere.

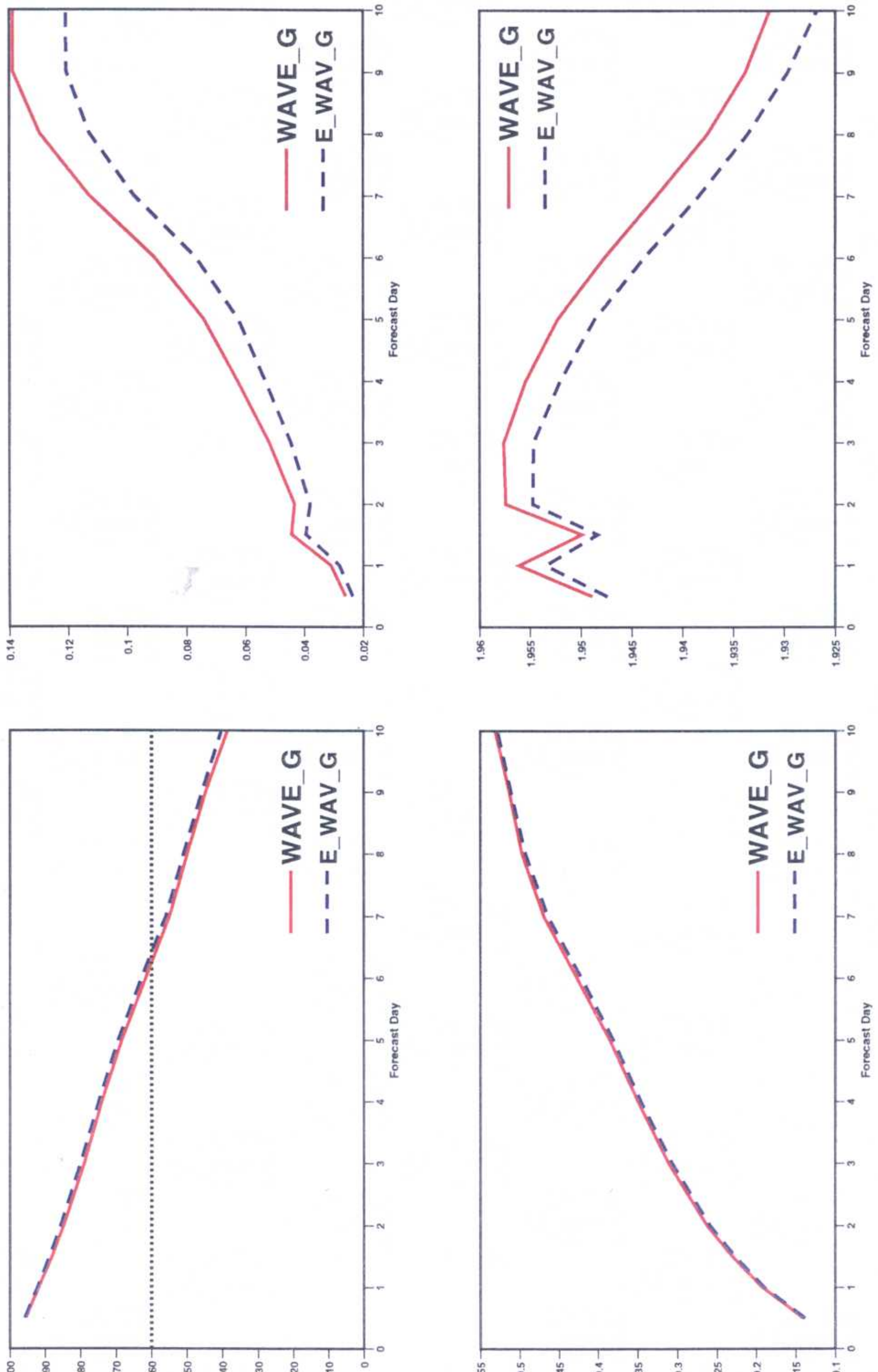

Fig. 12 (b) scores for the tropics.

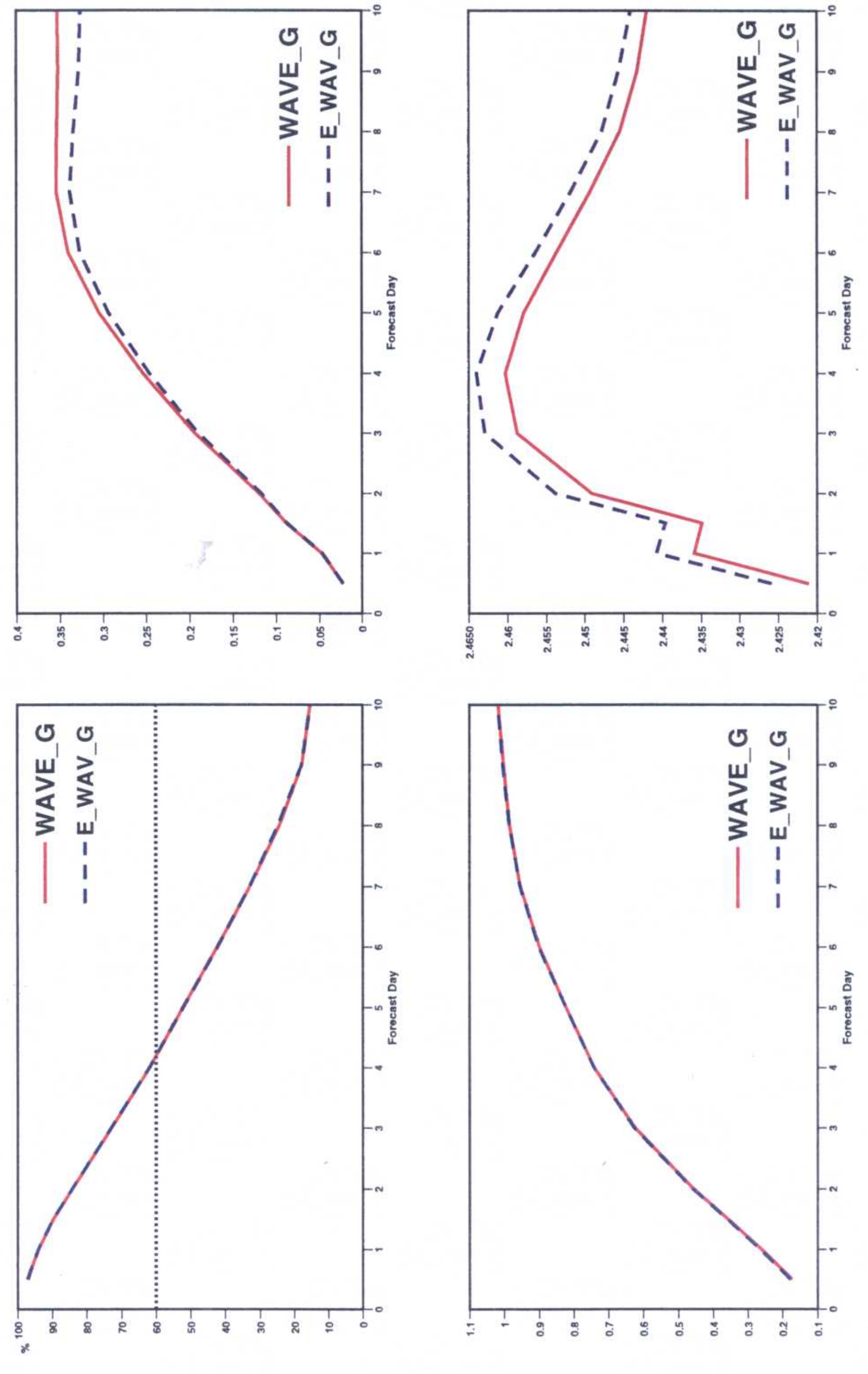

Fig. 12 (c) scores for the southern hemisphere.